New design of triplexer based on metal–insulator–metal plasmonic ring resonators

Yaw-Dong Wu (吳曜東)

Electronic Engineering of National Kaohsiung University of Applied Sciences, Kaohsiung 807, China

Corresponding author: ydwu@cc.kuas.edu.tw

Received August 27, 2014; accepted September 11, 2014; posted online October 28, 2014

In this work, we propose a new design of all-optical triplexer based on of metal–insulator–metal (MIM) plasmonic waveguide structures and ring resonators. By adjusting the radii of ring resonators and the gap distance, certain wavelengths can be filtered out and the crosstalk of each channel can also be reduced. The numerical results show that the proposed MIM plasmonic waveguide structure can really function as an optical triplexer with respect to the three wavelengths, that is, 1310, 1490, and 1550 nm, respectively. It can be widely used as the fiber access network element for multiplexer–demultiplexer wavelength selective in fiber-to-the-home communication systems with transmission efficiency higher than 90%. It can also be a potential key component in the applications of the biosensing systems.

OCIS codes: 060.1810, 130.7408, 130.3120, 230.5750.

doi: 10.3788/COL201412.110607.

Channel drop filter (CDF) is a communication component in which the optical signal is fed into one of the input ports and then the signal passes through the wavelength multiplexer of the CDF and finally emits at output port with almost no disturbance[1–3]. The CDF is composed of three parts: resonator system, bus waveguide, and drop waveguide. The incident electromagnetic wave propagates along the bus waveguide and certain frequencies will be dropped by resonator system to drop waveguide. The most common resonator system generally has a rectangle[4], ring, and disc resonator. In optical communication system, the CDF is useful and essential for triplexer filter. The three commonly used wavelengths are 1310, 1490, and 1550 nm, defined by ITU-T G.983 standard. Triplexer filter is widely used in fiber-to-the-home (FTTH) system, where 1310 nm channel is used for uploading data, 1490 nm channel is used for downloading data and voice, and 1550 nm channel is used for receiving video, respectively. Recently, many researchers have proposed surface plasmonic waveguide structures to design optical triplexers. The metal–insulator–metal (MIM) plasmonic structure consists of a dielectric waveguide and two metallic claddings, which strongly confine the incident light in the insulator region[5]. Some devices based on the MIM plasmonic waveguides have been studied numerically and experimentally, for example, the filters based on ring resonators[6], nanocavity resonators[7,8], tooth-shaped plasmonic waveguide filters[9–12], nanodisc resonators[13], and Y-shaped combiners[14]. Recently, Liu *et al.* proposed the plasmonic nanocavities and plasmonic arrays for promising applications in highly integrated optoelectronic devices, such as plasmonic biosensors, filters, and electro conductors[15–18]. Wang *et al.* proposed tunable multi-channel wavelength demultiplexer (WDM) based on MIM plasmonic nanodisc resonators at telecommunication regime and nanoplasmonic WDM based on MIM plasmonic waveguides[19,20]. They used nanodisc and rectangular resonators to design WDM structures. The transmission efficiency is about 50%–60%. Traditionally, WDMs have been proposed using the arrayed waveguide grating[21–23]. They have a major disadvantage, that is, they cannot be further miniaturized. Nowadays, many researchers have proposed using MIM plasmonic waveguides to solve this problem. In this work, the nanoring resonators and the MIM plasmonic waveguide structures are used to design the all-optical triplexer based on CDF. The proposed all-optical triplexer can filter out the 1310, 1490, and 1550 nm wavelengths. Those wavelengths can be used in FTTH with transmission efficiency higher than 90%. It can also be a potential key component in the applications of the biosensing systems.

In general, the interface between semi-infinite materials having positive and negative dielectric constants can effectively guide transverse magnetic (TM) surface waves. Because the width of the MIM plasmonic waveguide is much smaller than the wavelength, only the fundamental TM (TM_0) waveguide mode can propagate. The dispersion equation for TM mode in the waveguide is given by[24]

$$\varepsilon_d k_m + \varepsilon_m k_d \tanh\left(\frac{k_d}{2} w\right) = 0, \tag{1}$$

where k_d and k_m are defined as $k_d = (\beta^2 - \varepsilon_d k_0^2)^{\frac{1}{2}}$ and $k_m = (\beta^2 - \varepsilon_m k_0^2)^{\frac{1}{2}}$. ε_d and ε_m are the dielectric constants of the insulator and the metal, respectively. $k_0 = 2\pi/\lambda$ is the free-space wave vector. The propagation constant β is represented as effective index $n_{eff} = \beta/k_0$ of the waveguide for surface plasmon-polariton (SPP). In the work, the dielectric is assumed to be air with $\varepsilon_d = 1$,

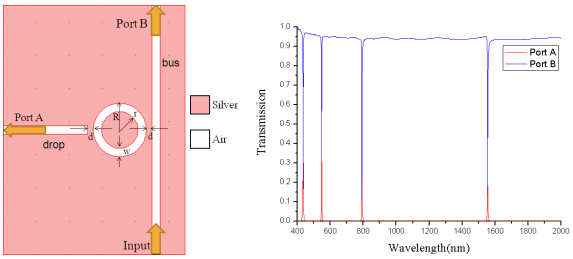

(a) (b)

Fig. 1 (a) CDF structure realized in MIM waveguides with a ring resonator. (b) Normalized transmission spectrum of the CDF.

and the metal to be silver. The dielectric constant ε_m of silver can be calculated by the Drude model[25]

$$\varepsilon_m(\omega) = \varepsilon_\infty - \frac{\omega_p^2}{\omega(\omega + i\gamma)}, \quad (2)$$

where ε_∞ stands for the dielectric constant at infinite angular frequency with the value of 3.7, $\omega_p = 1.38 \times 10^{16}$ Hz is the bulk plasma frequency, which represents the natural frequency of the oscillations of free conduction electrons, $\gamma = 2.73 \times 10^{13}$ Hz is the damping frequency of the oscillations, and ω is the angular frequency of the incident electromagnetic radiation. The SPPs are excited with inputting a TM-polarized plane wave. The transmission of the structure is defined as $T = P_o/P_i$ where P_i presents the total input power and P_o is the total output power. The quality factor is defined as

$$Q = \frac{\lambda}{\Delta\lambda}, \quad (3)$$

where λ is the resonance wavelength of the ring resonator and $\Delta\lambda$ is the full-width at half-maximum (FWHM) of transmission spectrum[26]. First, two straight waveguides and a ring resonator are used to construct a CDF based on MIM waveguide structure (Fig. 1(a)). The parameters of the structure are set to be $w = 50$ nm, $d = 35$ nm, $r = 155$ nm, and $R = 205$ nm. When the input optical signals contain multiple wavelengths, only the optical signals with the resonant wavelengths can propagate through the MIM plasmonic ring resonator waveguide structure. Hence a MIM plasmonic ring resonator waveguide structure can have several resonant modes (Fig. 1(b)). When the optical signals are launched from the input port, most of the optical signals directly propagate through the output Port B and only the optical signal with specific frequencies can be dropped to the output Port A by the ring resonator. The transmission spectrum of the CDF structure realized in MIM plasmonic waveguides with a ring resonator is shown in Fig. 1(b). Figure 1(b) shows that there are four resonant modes wherein specific frequencies can be dropped to the output Port A. Three resonant modes are in the visible light region and only one resonant mode is in the infrared light region. In this work, the wavelengths of incident light are chosen in the infrared region. From the simulation results, one resonance peak at the wavelength $\lambda = 1554$ nm is located in the range of 1250–1600 nm, and the corresponding maximum transmission efficiency is 38.2%. The quality factor at 1554 nm is 777 in the case of $d = 35$ nm. Figure 2 shows a nearly linear relationship between the radii of ring resonators and the transmitted peak wavelengths. By properly choosing the values of the radii of the ring resonators, the transmitted peak wavelengths of the MIM plasmonic optical filters can be tuned in the infrared region or in the visible light region. The dropped central peak wavelengths are listed in Table 1. Figure 3(a) shows the transmission spectrum for the ring resonator with $R = 205$ nm, $r = 155$ nm, and $w = 50$ nm for different gap distances. When the gap distance d is 25 nm, one resonance peak was observed at the wavelength $\lambda = 1561$ nm. The corresponding maximum transmittance is about 40.64% and the quality factor is 260. For other gap distances $d = 30$, 35, 40, and 45 nm, the corresponding resonance peak wavelengths are at $\lambda = 1557$, 1554, 1553, and 1552 nm, respectively, the respective maximum transmittances are 39.6%, 38.2%, 33.5%, and 31.2%, and the quality factors are 389, 777, 1035, and 1410, respectively. Figure 3(b) shows that as the gap distances increase, the peak wavelength decreases. By properly adjusting the gap distance, the quality factor can be greatly improved, whereas the transmission efficiency cannot be improved at all. To improve the transmission efficiency, a reflector was introduced at the end of the output Port B (Fig. 4(a)). The reflective length L is the length between a reflector and the drop waveguides. The transmission spectrum is shown in Fig. 4(b). In the case of without the reflector, the peak wavelength is at 1554 nm and the corresponding maximum transmittance is 38.2%. In the case of with the reflector, the peak wavelength is at 1554 nm and the corresponding maximum transmittance is 51.6%. By putting the reflector, the transmission efficiency can be improved about 13%. But this is still not good enough, trying to adjust the reflective length L is another method to enhance the transmission efficiency. For the three-port CDF, high channel drop efficiency can be achieved if the resonators are properly located from the reflector[27]. As shown in Fig 5(a), the reflective length is adjusted from 0 to 300 nm with $R = 205$ nm, $r = 155$ nm, and $d = 45$ nm. The numerical results

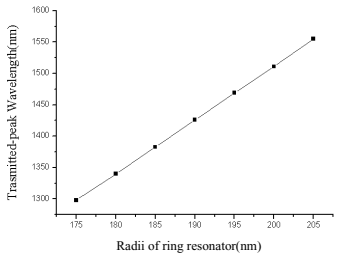

Fig. 2. Transmitted-peak wavelength of the filter versus the radius of the ring resonator.

Table 1. Wavelength of Dropping Range corresponding to Different Resonator Sizes

Ring Resonator of Size (nm)	Drop Wavelength of Range (nm)	Central Wavelength (nm)
175	1296–1300	1298
180	1339–1342	1340
185	1382–1384	1383
190	1425–1427	1426
195	1468–1470	1469
200	1510–1514	1511
205	1554–1556	1555

show that the optimum transmission efficiencies are at $L = 300$ nm, the peak wavelength is at 1552 nm, and the corresponding maximum transmittance is 95.87%. As shown in Fig. 5(b), the reflective length is adjusted from 0 to 300 nm with $R = 177$ nm $r = 127$ nm, and $d = 45$ nm. The numerical results show that the optimum transmission efficiencies are at $L = 100$ nm, the peak wavelength is at 1312 nm, and the corresponding maximum transmittance is 95.23%.

Four straight waveguides and three ring resonators were used to construct an all-optical triplexer based on MIM plasmonic waveguide structure (Fig. 6(b)). Before designing the triplexer, the influence of the separation length between two ring resonators must be investigated first. In Fig. 6(a), three straight waveguides and two different radii of ring resonators are used to find out the influence. The parameter L_1 is designated as the separation length between the first and the second ring resonators, and the parameter L_2 is designated as the separation length between the second and the third ring resonators. The separation length L_i is an important parameter, which introduces a phase difference between the two ring resonators, thus influencing the transmission characteristics of the proposed all-optical triplexer[28]. The parameters of the structure are set to be $L = 300$ nm, $R_1 = 205$ nm, $R_2 = 198$ nm, $w = 50$ nm, and $d = 45$ nm. In Fig. 7(a), the first ring resonator drops

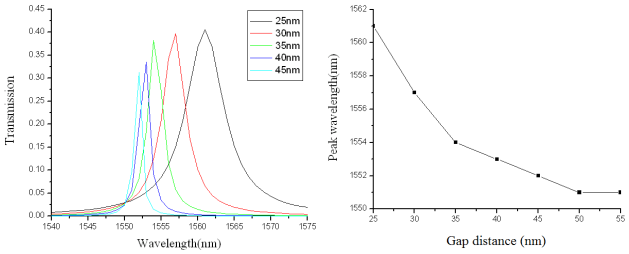

(a) (b)

Fig. 3 (a) Transmission spectra for different gap distance d with $R = 205$ nm, $r = 155$ nm, and $w = 50$ nm. (b) Transmitted peak wavelength versus gap distance d.

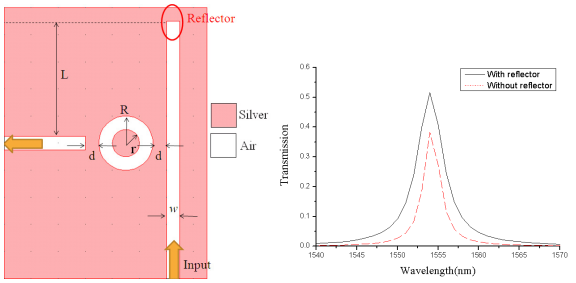

(a) (b)

Fig. 4 (a) CDF structure with reflector. (b) Transmission spectra with reflector and without reflector.

peak wavelength at $\lambda_1 = 1550$ nm and the transmittance is only 12.38%. The second ring resonator drops peak wavelength at $\lambda_2 = 1490$ nm and the transmittance is only 5.17%. When $L_1 = 400$ nm, the simulation results are very bad. In Fig. 7(b), the transmission of the first ring resonator is 90.06% and the second ring resonator is 42.6%. When $L_1 = 450$ nm, the transmission efficiency is improved. But the transmission of the second ring resonator is still too low. In Fig. 7(c), the transmission of the first ring resonator is 90.17% and the second ring resonator is 91.98%. When $L_1 = 500$ nm, one can see that both of the first and second ring resonators have the best transmittances. In Fig. 7(d), the transmission of the first ring resonator is 89.93% and the second ring resonator is 72.61%. When $L_1 = 550$ nm, the first ring resonator still has good transmittances, whereas the second ring resonator's efficiency is reduced

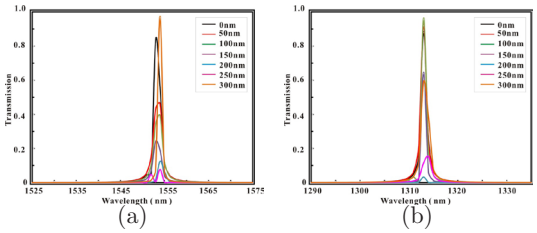

(a) (b)

Fig. 5. Transmission spectra for different reflective length L with $d = 45$ nm and $w = 50$ nm: (a) $R = 205$ nm and (b) $R = 177$ nm.

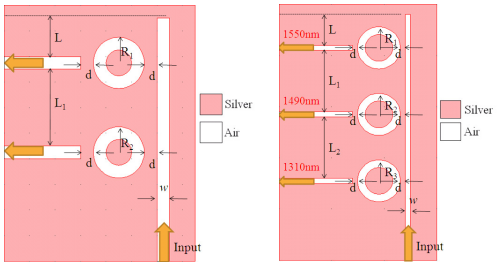

(a) (b)

Fig. 6 (a) MIM waveguide consisting of two ring resonators with different radii R_1 and R_2. (b) Schematic of the proposed all-optical triplexer.

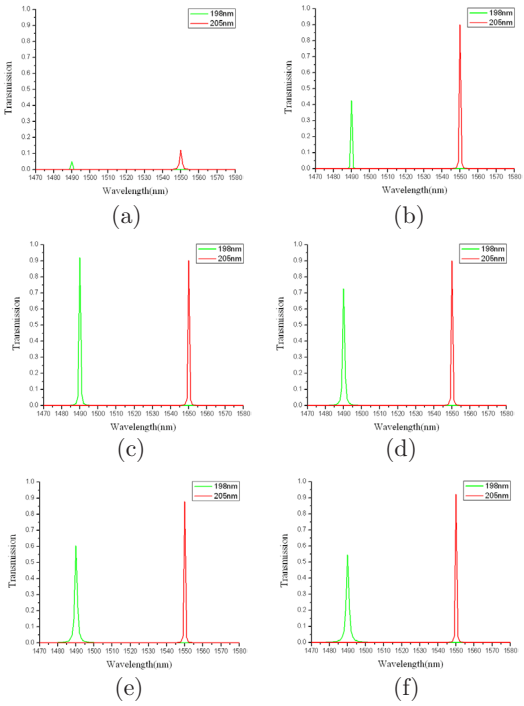

Fig. 7. Transmission spectra for fixed $L = 300$ nm, $R_1 = 205$ nm, and $R_2 = 198$ nm with different L_1: (a) 400, (b) 450, (c) 500, (d) 550, (e) 600, and (f) 650 nm.

to about 19.37%. In Fig. 7(e), the transmission of the first ring resonator is 87.83% and the second ring resonator is 60.43%. In Fig. 7(f), the transmission of the first ring resonator is 92.18% and the second ring resonator is 54.53%. According to the simulation results, the optimal distance is $L_1 = 500$ nm. Next, the same method is used to investigate the influence between each two ring resonators. The optimal parameters of the proposed MIM plasmonic all-optical triplexer are chosen as: $R_1 = 205$ nm, $R_2 = 198$ nm, $R_3 = 177$ nm, $L = 300$ nm, $L_1 = 500$ nm, $L_2 = 650$ nm, $w = 50$ nm, and $d = 45$ nm. The transmission spectrum of the MIM plasmonic all-optical triplexer is shown in Fig. 8(a). The dropped peak wavelengths of ring resonators are $\lambda_1 = 1550$ nm, $\lambda_2 = 1490$ nm, and $\lambda_3 = 1310$ nm, respectively, and the transmission efficiencies are 91.48%, 95.42%, and 96.55%, respectively. The field distributions of the proposed all-optical triplex for wavelengths of 1550, 1490, and 1310 nm are shown in Figs. 8(b)–(d).

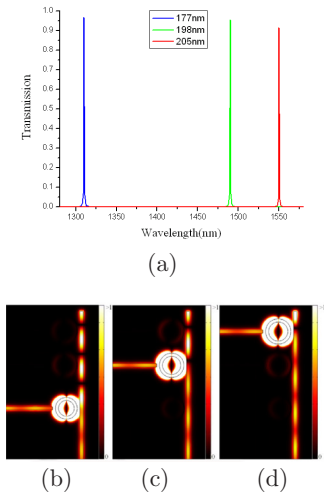

Fig. 8 (a) Transmission spectra of the triplexer filter. Field distributions of $|Hz|$ with incident wavelengths of: (b) 1310, (c) 1490, and (d) 1550 nm.

In conclusion, a new type of MIM plasmonic all-optical triplexer has been proposed. It is composed of three straight waveguides and two different radii of ring resonators. By properly turning the radii of ring resonators and the gap distance, certain wavelengths can be filtered out and the crosstalk of each channel also can be reduced. As the numerical results shown above, it could really function as an optical triplexer with respect to the three wavelengths i.e. 1310, 1490, and 1550 nm, respectively. It would also be a potential key component in the applications of the FTTH communication systems and the biosensing systems.

The author thanks Yung-Ta Hsueh for his constructive discussion and help.

References

1. S. S. Xiao, L. Liu, and M. Qiu, Opt. Express **14,** 2932 (2006).
2. C. Manolatou, M. J. Khan, S. Fan, P. R. Villenueve, H. A. Haus, and J. D. Joannopoulos, J. Quant. Electron. **35,** 1322 (1999).
3. B. E. Little, S. T. Chu, H. A. Haus, J. Foresi, and J. P. Laine, J. Lightwave Technol. **15,** 998 (1997).
4. A. Hosseini and Y. Massoud, in *Proceedings of IEEE Conference on Nanotechnology* 81 (2007).
5. G. Veronis, Z. Yu, S. E. Kocabas, D. A. B. Miller, M. L. Brongersma, and S. Fan, Chin. Opt. Lett. **7,** 302 (2009).
6. T. Wang, X. Wen, C. Yin, and H. Wang, Opt. Express **17**, 24096 (2009).
7. Z. Chen, J. Chen, Y. Li, J. Qian, J. Qi, J. Xu, and Q. Sun, Chin. Opt. Lett. **11,** 112401 (2013).
8. Y. Shen, G. Yu, J. Fu, and L. Zou, Chin. Opt. Lett. **10,** 021301 (2012).
9. J. Tao, X. Huang, X. Lin, Q. Zhang, and X. Jin, Opt. Express **17,** 13989 (2009).
10. J. Tao, X. Huang, X. Lin, J. Chen, Q. Zhang, and X. Jin, J. Opt. Soc. Am. B **27,** 323 (2010).
11. X. Lin and X. Huang, J. Opt. Soc. Am. B **26,** 1263 (2009).
12. X. Lin and X. Huang, Opt. Lett. **33,** 2874 (2008).
13. H. Lu, X. M. Liu, D. Mao, L. R. Wang, and Y. K. Gong, Opt. Express **18,** 17922 (2010).
14. H. Gao, H. Shi, C. Wang, C. Du, X. Luo, Q. Deng, Y. Lv, X. Lin, and H. Yao, Opt. Express **13,** 10795 (2005).
15. Z. Q. Liu, G. Q. Liu, H. Q. Zhou, X. S. Liu, K. Huang, Y. H. Chen, and G. Fu, Nanotechnol. **24,** 155203 (2013).
16. Z. Q. Liu, G. Q. Liu, K. Huang, Y. H. Chen, Y. Hu, X. N Zhang, and Z. J. Cai, IEEE Photon. Technol. Lett. **25,** 1157 (2013).
17. G. Q. Liu, Y. Hu, Z. Q. Liu, Y. H. Chen, Z. J. Cai, X. N Zhang, and K. Huang, Phys. Chem. Chem. Phys. **16,** 4320 (2014).
18. Z. Q. Liu, H. B. Shao, G. Q. Liu, X. S. Liu, H. Q. Zhou, Y. Hu, X. N. Zhang, Z. J. Cai, and G. Qu, Appl. Phys. Lett. **104,** 081116 (2014).
19. G. Wang, H. Lu, X. Liu, D. Mao, and L. Duan, Opt. Express **19,** 3513 (2011).

20. H. Lu, X. Liu, Y. Gong, D. Mao, and G. Wang, J. Opt. Soc. Am. B **28,** 1616 (2011).
21. X. Li, G. R. Zhou, N. N. Feng, and W. P. Huang, IEEE Photon. Technol. Lett. **17,** 1214 (2005).
22. C. Xu, X. Hong, and W. P. Huang, Opt. Express **14,** 4675 (2006).
23. T. Lang, J. J. He, and S. He, IEEE Photon. Technol. Lett. **18,** 232 (2006).
24. J. A. Dionne, L. A. Sweatlock, H. A. Atwater, and A. Polman, Phys. Rev. B **73,** 035407 (2006).
25. Z. Han, E. Forsberg, and S. He, IEEE Photon. Technol. Lett. **19,** 91 (2007).
26. B. Wang and G. P. Wang, Appl. Phys. Lett. **87,** 013107 (2005).
27. S. Kim, I. Park, and H. Lim, Opt. Express **12,** 5518 (2004).
28. H. Lu, X. Liu, and D. Mao, Phys. Rev. A **85,** 053803 (2012).